Konya Mühendislik Bilimleri Dergisi, c. 12, s. 2, 542-560, 2024
Konya Journal of Engineering Sciences, v. 12, n. 2, 542-560, 2024
ISSN: 2667-8055 (Electronic)
DOI: 10.36306/konjes.1449969

LITHIUM EXTRACTION POTENTIAL OF HECTORITES FROM THE BIGADIÇ BORATE BASIN: MINERALOGICAL CHARACTERIZATION AND SELECTIVE CATION EXCHANGE EXPERIMENTS

***Hatice ÜNAL ERCAN**

Konya Technical University, Vocational School of Technical Sciences, Chemistry and Chemical Processing Technologies, Konya, TÜRKİYE
hunalercan@ktun.edu.tr

Highlights

- The mineralogical characteristics of the clays in the Bigadiç borate basin have been assessed.
- Selective cation exchange of hectorite with various cations was investigated.
- Mg and Li concentrations transferring from clay to acidic solution were ascertained.
- Experimental observations were conducted based on the ions' diameters and hydration enthalpy.
- Partition coefficient values were calculated from solutions and interpreted.

Graphical Abstract

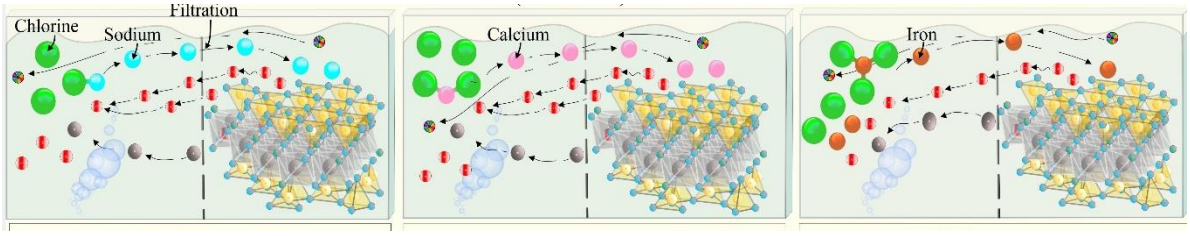

Model showing the process of Li extraction from hectorite with cations of different ionic charges.

***Corresponding Author**: Hatice ÜNAL ERCAN, hunalercan@ktun.edu.tr

Konya Mühendislik Bilimleri Dergisi, c. 12, s. 2, 542-560, 2024
Konya Journal of Engineering Sciences, v. 12, n. 2, 542-560, 2024
ISSN: 2667-8055 (Electronic)
DOI: 10.36306/konjes.1449969

LITHIUM EXTRACTION POTENTIAL OF HECTORITES FROM THE BIGADIÇ BORATE BASIN: MINERALOGICAL CHARACTERIZATION AND SELECTIVE CATION EXCHANGE EXPERIMENTS

***Hatice ÜNAL ERCAN**

Konya Technical University, Vocational School of Technical Sciences, Chemistry and Chemical Processing Technologies, Konya, TÜRKİYE
hunalercan@ktun.edu.tr

(Received: 09.03.2024; Accepted in Revised Form: 03.05.2024)

ABSTRACT: Although lithium is a common element worldwide, it is primarily concentrated in specific areas, including pegmatites, granites, and clays, as well as brine. Today, research in various countries is exploring experimental techniques for extracting Li from Li rich rocks and clays. The Bigadiç boron deposits form in a volcano-sedimentary environment in western Turkey, and their boron minerals interlayer with significant amounts of Li-rich hectorite. However, the clays' high Mg content presents a significant complication, increasing the cost of lithium processes and necessitating an intricate extraction process.

In this study, a solution with high Li and low Mg content was obtained by a two-step extraction process from raw Bigadiç clays with high Li content. Raw hectorite samples NaCl, $CaCl_2$ and $FeCl_3$ cation sources were mixed by the mechanical mixing method to provide cation absorption on the clay surface. The targeted ion, Li, was transferred from the clay to the solution by preferential displacement using acid treatment. The findings produced through D_{Li} =[$Li_{(clay)}$]/[$Li_{(aq)}$] (ppm/ppm) and logD_{Li}= 1319/$T_{(K)}$ + 5.5 ([$Li_{(aq)}$]) $^{-0.0806}$ formulae were analyzed and interpreted. The investigation has demonstrated the viability of selective cation exchange procedures upon rich lithium clay reserves present in Bigadiç.

Keywords: *Bigadiç Borate Deposit, Clay Minerals, Hectorite, Lithium Extraction, Selective Cation Exchange*

1. INTRODUCTION

In recent years, the significance of lithium (Li) in the global market has risen due to advancements in technology that utilize Li's high electrochemical potential, leading to a corresponding rise in its price [1-3]. The utilization of rechargeable lithium batteries, particularly for eco-friendly electric/hybrid vehicles, is a significant factor in making lithium a reliable and useful material/source, therefore, as it produces no pollutants and meets the objectives of sustainable environmental policies. However, the demand for lithium is dramatically growing, and it is becoming crucial for the comprehensive investigation and utilization of all available natural and artificial sources [4].

Although clays are found in restricted regions on the Earth's surface such as Turkey, France, Morocco, Arizona and Nevada, they can possess large amounts of Li in their crystal structures, serving as a potential source of the Li element. However, understanding and predicting clay crystal systems poses a challenge due to the reactions of clay minerals which release cations by exchange or solution and the existence and diversity of exchangeable cations. Additionally, another difficulty is the existence of varying binding energies of these cations to different exchange sites located on clays [5-7].

Hectorite (Na0.6Mg2.7Li0.3Si4O10(OH)2), widely recognized as an adsorbent, catalyst, and rheological additive, and its use has lately increased in fields such as optics, medical materials, and tissue engineering is a smectite group magnesium-lithium clay mineral. Hectorite with the chemical formula $Na_{0.6}Mg_{2.7}Li_{0.3}Si_4O_{10}(OH)_2$ has a Si-O-Mg(Li)-O-Si layered trioctahedral structure separated by interlayer cations, such as Na+, and Li+. The adjacent negatively charged 2:1 layer is fixed by interlayer cations and by hydrogen bonding between water molecules coordinated to interlayer cations and basal oxygen atoms of the tetrahedral sheets. The partial isomorphic substitution of Li^+ for Mg^{2+} in the octahedral sheets is

***Corresponding Author**: Hatice ÜNAL ERCAN, hunalercan@ktun.edu.tr

responsible for the negative charges of hectorite. These negative charges are compensated by the interlayer cations in the interlayer space and interlayer cations can also be exchanged with other cations. Additionally, hectorite nanolayers exhibit an anisotropic charge distribution, with negative charges on the basal faces and positive charges on the edges [8, 9]. In addition to these characteristics, hectorite can be defined as a highly functional nanoparticle that can be used in cation exchange reactions with a high cation exchange capacity (CEC) of 50-150 mmol/100 g in the pH range of 6-13 [8]. and a large specific surface area of about 350 m^2/g [10]. The positioning and quantity of lithium in the crystal site must be clearly defined in the extraction of the Li element from hectorite or Li-rich clays. This is because Li^+ can occupy two distinct sites in the clay: i) Li+ substituting for Mg^{2+} in the structural octahedral sites, and ii) exchanged Li^+, a cation that is primarily located in the interlayer sites and is exchangeable [11]. It is essential to ensure that these two sites are distinguished from each other. It is believed that the replacement of Mg^{2+} with Li^+ in the octahedral sites is a result of the element's position in the periodic table and their closely linked external geochemical cycles [12, 13].

Many studies have revealed that besides inorganic ions, organic cations can also be incorporated into the interlayer space of hectorite through an ion-exchange reaction [14-22]. Bivalent cations are much more likely to enter the exchange sites than monovalent cations [23]. The treatment of rare-earth element and Li rich clay group minerals to be exploited for these elements are based on the fact that the charge on clay minerals is predominantly negative, attracting cations from solutions to neutralize the said charge. Ion exchange in these minerals occurs through a reversible chemical reaction between the ions in the solutions and the ions positioned on the crystal surface due to the unbalanced electrical charges within the crystal framework. Ion exchange reactions follow the law of mass action; however, the reactions are constrained by the count of exchange sites on the mineral and the strength of the bond between the exchangeable cations and the mineral surface [7, 24-28]. Hectorite possesses several active sites utilized for cation exchange, including interlayer, surface, edge, and inter-particle sites for conducting the ion-exchange reaction as outlined above. These active sites enable the clay to interact with other substances readily, leading to diverse types of reactions. This unique property allows for the manipulation of the hectorite's structure and functionality [9].

The Borate Basin around Bigadiç in Western Anatolia is extensively recognized with its Miocene borate deposits attracting widespread interest. On-going explorations and exploitation activities in the basin revealed the clay layers of the deposits are Lithium-rich [29-36]. The initial investigation of Li leaching was conducted by [37] utilizing sulfuric acid solution from ulexite-clay samples sourced from the Kırka borate deposit, including dolomite, montmorillonite, and hectorite. Despite favorable leaching conditions, this study highlighted that acid leaching failed to exhibit discernible Li selectivity (99%) and led to significant dissolution of iron (42.97%), magnesium (58.10%), and calcium (35.04%). With the advancement of technology new research was conducted, including new processes to obtain a solution rich in the element Li, and a very rich Li solution was obtained, but the biggest technical problem was that the solution was enriched with elements such as Mg and Ca at the same time as Li [34, 35]. Regarding the usefulness of grain size reduction, [36] also conducted a study and found that when grinding samples of different grain sizes and compositions, the amount of Li increased with decreasing grain size, while the increase in the amount of Li was associated with clay minerals.

All of the above indicates that we have entered a period of significant investment in lithium mining and production worldwide and in Turkey. Furthermore, it seems inevitable that lithium will open new dimensions in the economic and political fields as a result of international trade predictions. The growing economic and geopolitical significance of this raw material has attracted global attention to the boron basins in Turkey. The principal challenge encountered during the extraction of lithium from clays in Boron basins in Turkey is the co-extraction of magnesium. This study aims to develop a lithium-rich magnesium-poor solution during the extraction of lithium from clays. The findings of this study demonstrate the feasibility of obtaining a Li-rich, Mg-poor solution in the preliminary stages of extracting this raw material. For this purpose, unlike previous research, the clay samples were mixed and ground with a cation source before being mixed with acid. Additionally, the focus of the research was on the extraction of lithium

between the layers rather than on the octahedral layer. NaCl, $CaCl_2$ and $FeCl_3$ salts were blended and grinded as cation sources with Li-rich clays. In addition, the partition coefficient values of the geochemical data were calculated, evaluated and interpreted to support the integrity of the data and the applicability of the study.

1.1 Geology of the Bigadiç Borate Basin

The NE-SW-trending Bigadiç Borate Basin is classified as among the boron-rich basins in Western Anatolia (Figure 1). It covers an area of approximately 50-90 km and deposited over an amalgamated basement consisting of tectonic units of the Menderes Massif, the Sakarya Zone, the Lycian Nappes, and the Bornova Flysch Zone. The area experienced extensional deformation starting from the latest Oligocene as being a part of the Aegean Extensional province [38-42]. Miocene is remarkable with the development of the NE- and SW-trending basins as manifestations of a highly attenuated lithosphere and accompanied volcanism [43, 44]. These basins were filled with deposits eroded from highlands and produced by the surrounding volcanoes (Figure 1). The Neogene volcano-sedimentary sequences from bottom to top; basement volcanic unit, basement limestone unit, lower tuff unit, lower borate unit, upper tuff unit, upper borate unit and basalt [38]. (Figure 1, stratigraphic section). Quaternary sediments cover all these Neogene units.

Within the Miocene units of the Bigadiç Basin lie four open pits that are renowned worldwide as containing the largest colemanite and ulexite deposits: Simav, Tülü, Acep, and Avşar quarry (Figure 1). These deposits were formed due to Tertiary-Quaternary volcanic activity and are distinguished by the presence of borate minerals [40, 41]. Borate minerals are operated from two distinct section, upper and lower. In the lower section, the units enriched in borate minerals consist of intercalations of clayey limestone, marl, claystone, mudstone and tuff. In the upper section, the lithological sequence is very closely similar to that of the lower section, where units such as limestone, claystone, clayey limestone, marl and tuff are intercalated [30, 41] (Figure 1, stratigraphic section, left). This study used samples from the upper borate zone of the Simav quarry. The Simav quarry represents the basin's deeper parts, with Ca- and Na-borates (colemanite + ulexite) being the predominant borate minerals present in Simav (Figure 1. stratigraphic section, right). Clays of the quarries intercalate with other sediments in borate-rich strata, and these clays indicate considerable quantities of the element Li. Li in borate deposits in the region is mostly confined to clay minerals, and studies of clays have shown that the clays in this region contain between 0.17 and 0.58% Li_2O [31].

2. MATERIAL AND METHODS

The experimental studies were carried out in two stages. The first process is based on the characterization and determination of clays. The second process involves mixing clays with a cation source in a high-energy mill and obtaining a lithium-rich solution with the addition of a solvent.

2.1 Characterization of Clays

The clay samples (BG1, BG2 and BG3) were first cleaned of coarse gravel and sand-sized materials and boron minerals to obtain a purer clay composition. Then, the decantation technique, also known as suspended particle gravity sedimentation, was used to separate silt and clay-sized materials. < 2 μm clays were obtained by centrifugation from the dispersion obtained after the decantation process. An oriented aggregate mount was prepared for each clay sample prior to X-Ray diffraction (XRD). The oriented aggregate mounts force the clay mineral particles, usually plate-shaped phyllosilicates, to lie flat, allowing the incident X-ray beam to be directed along the z-axis of the minerals and the diagnostic basal diffraction to be recorded. Oriented samples were air dried, then solvated with ethylene glycol (EG) at 60°C for 2 hours and thermally heated at 400°C and 550°C for 1/2 hour. All these steps are the basis for the

determination of the mineralogical composition of clays <2 μm. XRD analyses were performed at Konya Technical University, Central Laboratory Application and Research Center, Konya, Turkey, in GNR EUROPE 600 XRD model device, CuKα radiation, 40 mA, 40 kV operating conditions, 0.005° scanning speed, 0.250 mm slit interval. The 2θ range was preferred as 2.0–45.0° for EG-solvated and thermally treated samples.

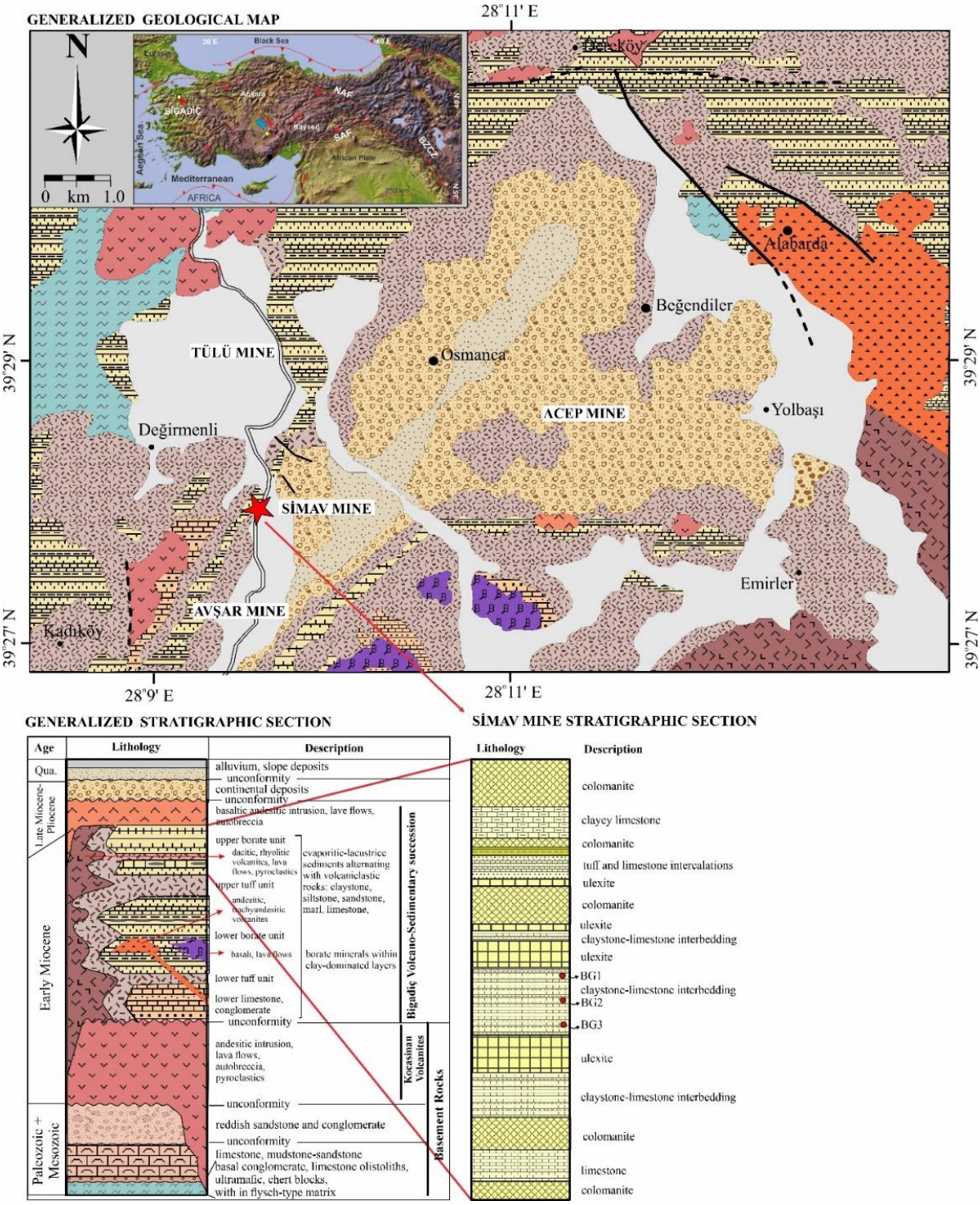

Figure 1. Generalized geological map and stratigraphic section (without scale) of Bigadiç Borate Basin, (the formation colors correspond to the generalized stratigraphic section) (Modified from [30, 41]).

The cation exchange capacities (CEC) of the clays were determined using the methylene blue technique. The technique estimates the quantity of exchangeable cations present in reactive clays. The reaction in this method is the replacement of the methylene blue cations by exchangeable cations of the clay. Clay adsorbs methylene blue in the quantity of exchangeable cations. After saturation, the added methylene blue ions are released into the dispersion. Since the amount of methylene blue added is known, the amount of methylene blue adsorbed by the clay can be calculated and as a result, it can be said that the clay has a cation exchange capacity equal to the amount of charge adsorbed. In the present study, 3.20 g of methylene blue (C16H18N3SCI) was dissolved in 1L of water and thus 0.01 meq load was obtained in 1 cm3 volume [45]. The methylene blue solution was added to 1 g of dry clay in 0.5 ml volumes. After each addition of methylene blue, the clay was mixed and dripped from the dispersion onto the filter paper. The process was continued until the color left by pure methylene blue on the filter paper was formed around the clay dripped onto the filter paper. The cation exchange capacity of the clay was calculated from the amount of methylene blue that was added until the blue ring was formed around the clay.

Field emission scanning electron microscope (FE-SEM) analyses were performed to determine the micromorphological properties of the samples. The micromorphological analysis of clays was carried out using a ZEISS GeminiSEM 500 model scanning electron microscope at Necmettin Erbakan University, Science and Technology Research and Application Centre (BİTAM), Konya, Turkey. The operating conditions of the FE-SEM are 15 kV acceleration voltage, 5-15 mA current and 10-20 s counting time for each element. The iridium coating process was performed using a Leica EM ACE600 model spray coater at 0.06 nm/s at 23 °C, at 0.4 nm. Li and Mg contents of the clays were analyzed by ICP-OS, Perkin Elmer 7000 DV model instrument at Selçuk University, Advanced Technology Research and Application Center (İLTEK), Konya, Turkey.

2.2. The Lithium Extraction Process

To increase their surface area, lithium-containing clay samples (BG1, BG2 and BG3) were ground in a ball mill for 30 min. Three different cation sources with different cation charges were used to perform the cation exchange in the Li extraction process, these are: sodium chloride (NaCl), calcium chloride ($CaCl_2$) and ferric chloride ($FeCl_3$) (Figure 2.). The anion of the cation source was selected from the halide combinations in all experimental groups. These cations were chosen mainly because their ion diameters and enthalpies of hydration (Δ_{Hhyd}) were different from each other, and thus ions with different physicochemical properties were aimed to clearly observe the behavior of the ions during the extraction. In this experimental phase partially used the technique applied to cation exchange tested by Sun et al., (2021). In the experimental groups, the mass ratio of the cation source to the clay mineral is 1: 5. Each clay (Cl) sample were mixed with a cation source (CS), then Cl-SC (BG1-NaCl, BG1-$CaCl_2$, BG1-$FeCl_3$, BG2-NaCl, BG2-$CaCl_2$, BG2-$FeCl_3$, BG3-NaCl, BG3-$CaCl_2$, and BG3-$FeCl_3$) experimental groups formed (see Figure 2). It was then powdered in a ball mill for 2 hours to allow the cations to adsorb onto the clay surface and to obtain a homogeneous mixture. Nano-multimix X 50 S, high-energy ball mill with 50 mL chamber at the Biochemistry Laboratory of Selçuk University in Konya/Turkey, was used to grind, mix the samples, and increase their surface area. All processes involving mixing the clay with the cation source were collectively referred to as the " Process-A " (Figure 2).

3 g Cl-SC samples were taken from each group and mixed with 50 ml 1M sulfuric acid (A) (process-A) and Clay-Cation Source-Acid (Cl-CS-A) solution was prepared (Figure 2). This solution was sloshed in an Erlenmeyer flask at 90°C for 24 hours in an ultrasonic bath. After the sloshing procedure, the solutions were percolated with filter paper (pore size 0.45 μm) and each solution was named accordingly as shown in Figure 2. The mixing process of the Cl-CS-A was called the "Process-B". After all of these "Processes-A and B", chemical measurements were performed on the filtrate (Figure 2).

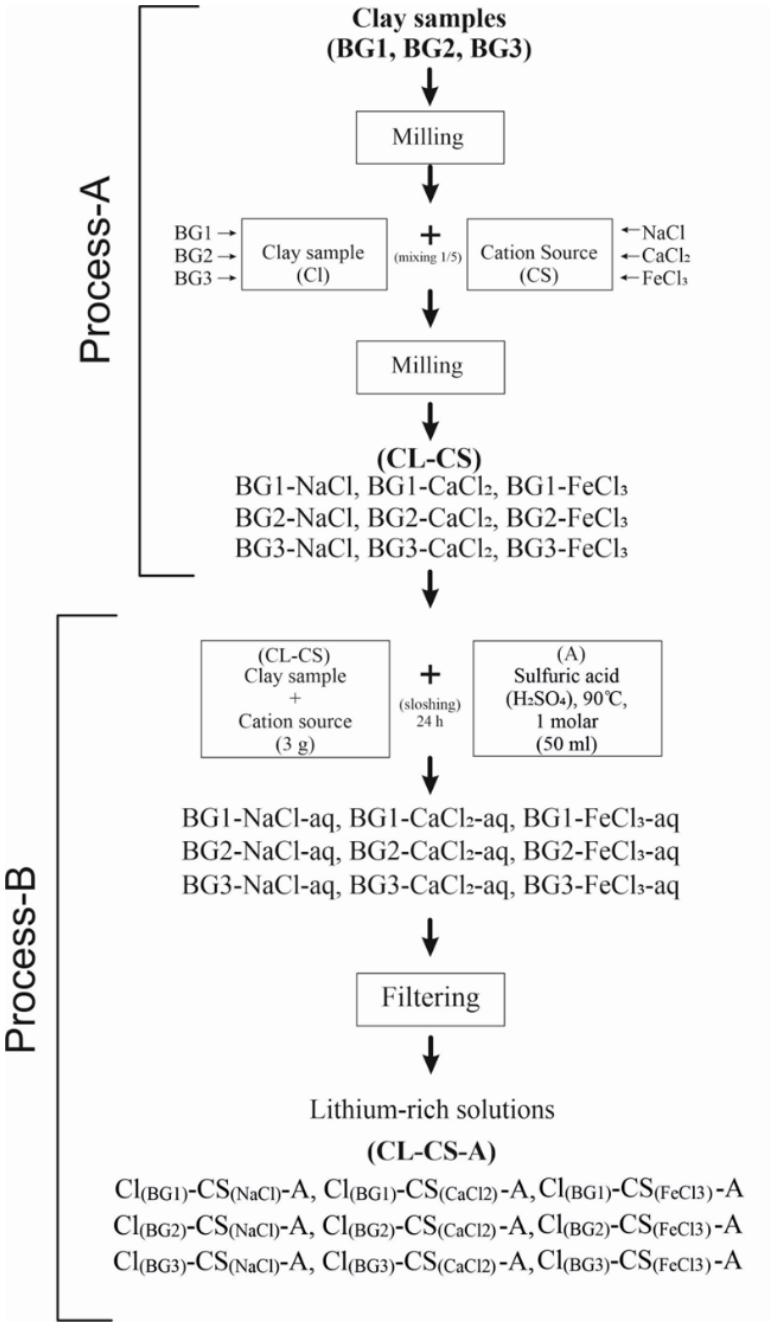

Figure 2. Flowchart outlining the methodology section, including the processes-A and B.

3. RESULTS

The mineralogical characterization of the Li-rich clay samples was carried out XRD analysis and is presented in Figure 3. After the treatment of the ethylene glycol (EG) on the clay sample, it was determined that at the XRD analysis the 001 reflection of the BG1 expanded from 13.01Å to 17.17Å, BG2 from 13.25Å to 17.29Å and the BG3 from 12.04Å to 16.73Å (Figure 3, left). After heating for 30m at 400 and 550 °C, the reflections were observed to have collapsed to about 9.5 to 10 Å. The 060 reflections from the randomly oriented XRD analysis of the samples were detected as 1.539 Å for BG1, 1.530 Å for BG2 and 1.528 Å for BG3 (Figure 3, middle).

The CEC of samples BG1, BG2 and BG3 was determined using the methylene blue cation exchange technique and was found to be 62 mmol/100 g, 54 mmol/100 g and 52 mmol/100 g respectively. In order

to determine the micromorphological structure of smectites, FE-SEM analysis was performed from BG1, BG2 and BG3 samples and wavy subhedral smectite flakes and irregular outlines were observed in each sample (Figure 3, right).

To determine the behavior of Li and Mg during the extraction of Li from the crystal structure of hectorite, the amount of Li and Mg elements was determined by chemical analysis. The Li contents of the raw clay samples (BG1, BG2 and BG3) are 2326.58 ppm, 1446.80 ppm and 1857.27 ppm, respectively. The Mg content is quite high and varies between 15.12%, 15.72% and 13.18% (Table 1).

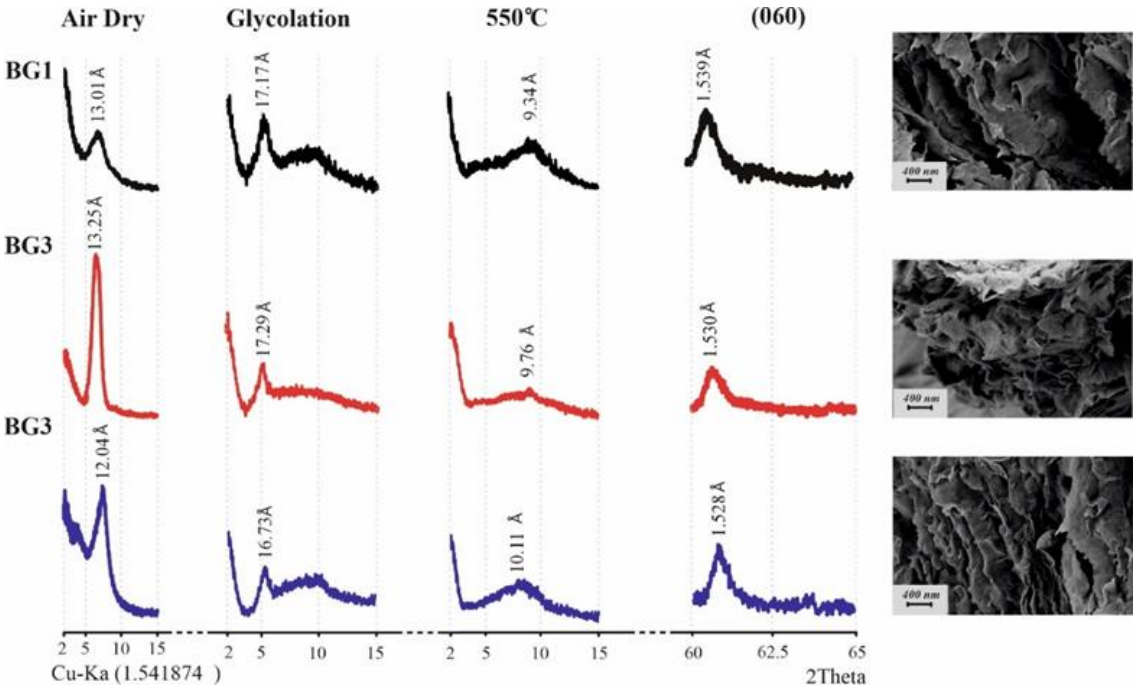

Figure 3. X-ray diffraction (XRD) patterns of clay-sized fractions separated from powdered clay samples at Bigadiç borate deposits Low-angle XRD patterns from 2θ: 2 to 15 ° for air-dried, ethylene-glycolate and thermally heated at 550°C vertically oriented to the c-axis of clay minerals at the left and middle. High angle XRD patterns from 2θ: 60 to 65° including 060 reflections from randomly oriented clay samples at right. FE-SEM images of the samples are shown to the right of the figure.

Table 1. The table displays the Li and Mg levels in the BG1, BG2, and BG3 clays and the clay-cation source-acid (Cl-CS-A) solutions.

	ppm (clay)	ppm (Cl-CS$_{(NaCl)}$-aq)	ppm (Cl-CS$_{(CaCl2)}$-aq)	ppm (Cl-CS$_{(FeCl3)}$-aq)	Recovery %(*)		
	BC1	BC1-NaCl-Aq	BC1-CaCl$_2$-Aq	BC1-FeCl$_3$-Aq	NaCl	CaCl	FeCl
Li	2326,5	1821,6	1652	603,3	78,29	71,00	25,93
Mg	151227,9	5443,3	6178,3	4249,1	3,59	4,08	2,80
	BC2	BC2-NaCl-aq	BC2-CaCl2-aq	BC2-FeCl3-aq			
Li	1446,8	843,3	990,5	457,1	58,28	68,46	31,59
Mg	157234,0	4271,5	4229,5	3901	2,71	2,68	2,48
	BC3	BC3-NaCl-aq	BC3-CaCl2-aq	BC3-FeCl3-aq			
Li	1857,2	1216,7	933,1	613,9	65,51	50,24	33,05
Mg	131810	4584,8	5031,63	4500,2	3,47	3,81	3,41

(*) The right three columns illustrate the percentages of Li and Mg elements that transition from the clay to the solution.

3.2 Chemical Composition and Extraction Process of Clays

The extraction of lithium-rich samples BG1, BG2 and BG3 were carried out through two separate steps, Process-A and Process-B (see Section the Lithium Extraction Process), further details of the procedure can

be found in [22]. Li and Mg concentrations were measured in all experimental groups following the processes-A and B. Among Cl-CS$_{(NaCl)}$-A solutions, the highest concentration of Li was obtained from Cl$_{(BG1)}$-CS$_{(NaCl)}$-A solution with 1821.6 ppm (Table 1). The Mg content of these solutions varies between 4271.5 ppm and 5443.3 ppm and increases in direct proportion to the Li content. The magnesium content of these solutions ranges from 4271.5 to 5443.3 ppm (Table 1). In Cl-CS$_{(CaCl2)}$-A solutions, the highest Li concentration was determined as 1652.0 ppm in Cl$_{(BG1)}$-CS$_{(CaCl2)}$-A solution. The Mg content of these solutions increases up to 6178.3 ppm. Li contents of Cl-CS$_{(FeCl3)}$-A solutions are quite low, varying between 457.1 ppm and 613.9 ppm. The Mg content of the same samples is ranging from 3901.0 ppm to 4249.1 ppm (Table 1) (Figure 4). As the Li content increases within the chemical composition of all solutions, so too does the Mg content. The percentage of Li and Mg transferred from clay into solution was calculated from the chemical data (Table 1). For all experimental groups, the percentage of Li transferred from the clay to the solution was quite variable, ranging from 78% (for Cl-CS$_{(NaCl)}$-A solutions) to 25% (for Cl-CS$_{(FeCl3)}$-A solutions) (Table 1) (Figure 4). For Cl-CS$_{(NaCl)}$-A solutions, the highest Li% was found in the Cl$_{(BG1)}$-CS$_{(NaCl)}$-A sample with 78%. Among the Cl-CS$_{(CaCl2)}$-A solutions, the highest Li content was found in the Cl$_{(BG1)}$-CS$_{(CaCl2)}$-A sample with 71%. The amount of Li% that was transferred from the Cl-CS(FeCl3)-A samples to the solution was detected to be quite low and was determined to be between 25% and 33% (Table 1) (Figure 4). For all experimental groups, the Mg% rate transferred from the clay to the solution was quite low and was calculated between 2.48% and 4.08% (Table 1, right). The rate of lithium release from clay into solution is quite high in comparison with magnesium and, proportionally, the amount of Mg increased as the amount of Li increased (Figure 4, left).

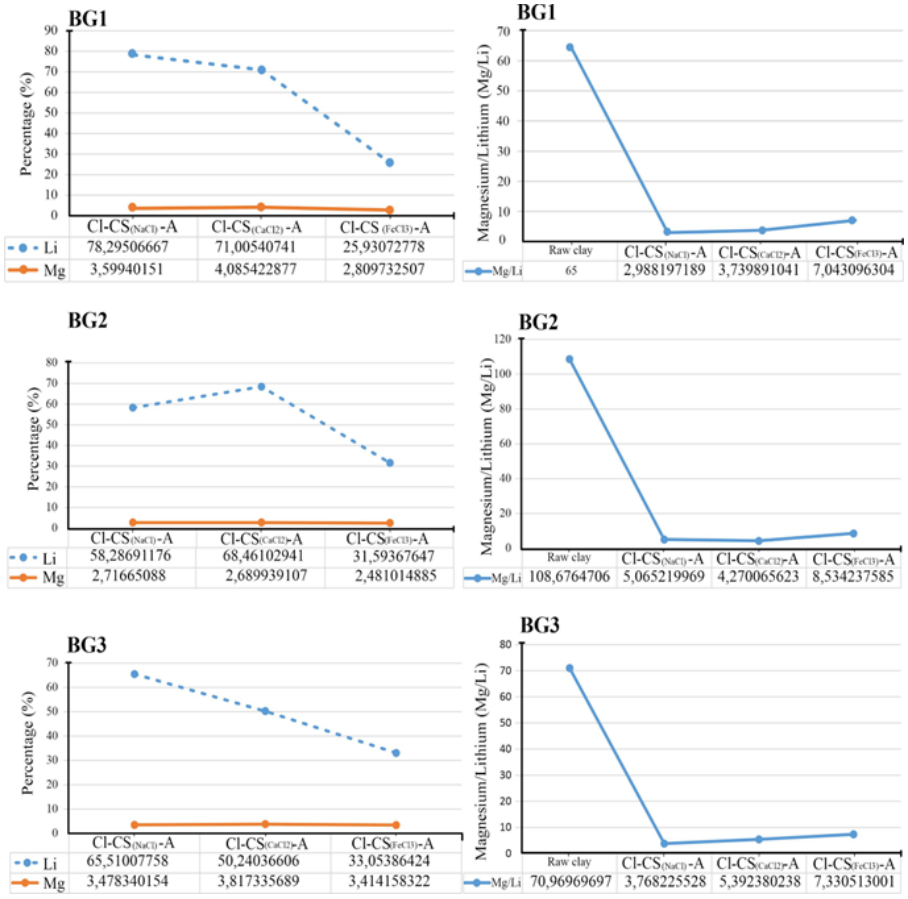

Figure 4. Graphs display the percentages of Li and Mg elements being released from clay minerals into Cl-CS-A solution (Left). Calculation is based on the ratio of Li content in solution to Li content in raw hectorite, and Mg content in solution to Mg content in raw hectorite. The Mg/Li ratios of raw clay and Cl-CS-A solutions (right).

The molar Mg/Li ratios of BG1, BG2 and BG3 clays are 65, 108.6 and 70.9 respectively. After applying the "A + B process", the molar Mg/Li ratio in the solutions decreased to 2.9 - 5.0 for Cl-$CS_{(NaCl)}$-A solutions, to 3.7 - 5 for Cl-$CS_{(CaCl2)}$-A solutions and to 7.0 - 8.5 for Cl-$CS_{(FeCl3)}$-A solutions (Table 2) (Figure 4).The Mg/Li ratios of the clays BG1, BG2, and BG3 were 65, 108.6, and 70.9, respectively. After applying the " process-A + B " with Cl-$CS_{(NaCl)}$-A, the Mg/Li ratio in the solutions for $Cl_{(BG1)}$-$CS_{(NaCl)}$-A, $Cl_{(BG2)}$-$CS_{(NaCl)}$-A and $Cl_{(BG3)}$-$CS_{(NaCl)}$-A decreased to 2.9, 5.0, and 3.7, respectively (Figure 4, right) (Table 2). The application of the " process-A+B " resulted in Mg/Li ratios ranging from 3.7 to 5.3 for Cl-$CS_{(CaCl2)}$-A solutions. Molar ratios of Mg/Li were calculated for the solutions $Cl_{(BG1)}$-$CS_{(FeCl3)}$-A, $Cl_{(BG2)}$-$CS_{(FeCl3)}$-A and $Cl_{(BG3)}$-$CS_{(FeCl3)}$-A, resulting in ratios of 7.0, 8.5 and 7.3 (Table 2) (Figure 4).

Table 2. The calculated Mg/Li ratios in BG1, BG2 and BG3 raw hectorite and the Cl-CS-A solutions.

Sample ID	Mg/Li Rations of Raw Clays	Mg/Li Rations of Solutions (Cl-$CS_{(NaCl)}$-A)	(Cl-$CS_{(CaCl2)}$-A)	(Cl-$CS_{(FeCl3)}$-A)
BG1	65,00	2,98	3,73	7,04
BG2	108,67	5,06	4,27	8,53
BG3	70,96	3,76	5,39	7,33

Table 3. Li and Mg contents of BG1, BG2, and BG3 raw hectorite samples and calculated partition coefficients of Li contents in Cl-CS-A solutions.

Raw Hectorite				Li partition coeff. ppm/ppm						Correction		
				D_{Li}			$D'_{Li/Mg}$			$\log D_{Li}$		
Sample ID	Li (ppm)	Mg (ppm)	Li/(Li+Mg) at./at.	Cl-$CS_{(NaCl)}$-A	Cl-$CS_{(CaCl2)}$-A	Cl-$CS_{(FeCl3)}$-A	Cl-$CS_{(NaCl)}$-A	Cl-$CS_{(CaCl2)}$-A	Cl-$CS_{(FeCl3)}$-A	Cl-$CS_{(NaCl)}$-A	Cl-$CS_{(CaCl2)}$-A	Cl-$CS_{(FeCl3)}$-A
BG1	2326	151227	0.015	1.277	1.408	3.856	0.045	0.057	0.108	9.211	9.114	8.106
BG2	1446	157234	0.009	1.715	1.460	3.165	0.046	0.039	0.078	8.441	8.602	7.828
BG3	1857	131810	0.013	1.526	1.990	3.025	0.053	0.075	0.103	8.808	8.542	8.123

$D_{Li} = [Li_{(clay)}]/[Li_{(aq)}]$, D'_{Li}-Mg = $([Li_{(clay)}]/[Mg_{(clay)}])/([Li_{(aq)}]/[Mg_{(aq)}])$, $\log D_{Li} = -1319/T(K) + 5.5\,([Li_{(aq)}])^{-0.0806}$

3.3 Calculation of Li partition coefficients in Cl-CS-A solutions

To interpret the data from the processes-A and B intelligibly, this study computes the partition coefficients of Li contents in Cl-CS-A solutions. Partition coefficients values are given in Table 3 and Figure 5, they are displayed either as $D_{Li}=[Li_{(clay)}]/[Li_{(aq)}]$(ppm/ppm) or $D'_{Li/Mg} = (Li/Mg)_{(clay)}/(Li/Mg)_{(aq)}$ (ppm/ppm) [11]. Depending on the cation source, the calculated D_{Li} and $D'_{Li/Mg}$ ratios vary (Figure 5). The ratio of D_{Li} for the Cl-$CS_{(NaCl)}$-A solutions of all the samples is between 1.27 and 1.71, while for the Cl-$CS_{(CaCl2)}$-A solutions it is between 1.40 and 1.99. In Cl-$CS_{(FeCl3)}$-A solutions the DLi ratio increases, varying between 3.02 and 3.85 (Table 3) (Figure 5). For Cl-$CS_{(NaCl)}$-A solutions the $D'_{Li/Mg}$ ratio is quite low, ranging from 0.04 to 0.05, while for Cl-$CS_{(CaCl2)}$-A solutions it is slightly increased to 0.04-0.07. The $D'_{Li/Mg}$ ratio increases up to 0.8-1.0 in Cl-$CS_{(FeCl3)}$-A solutions (Table 3) (Figure 5). A more general expression for the D_{Li} has been established by using the formula $\log D_{Li}$. This formula is known as Van't Hoff's law, which is $\log D_{Li}$ =

a103/T+b Van't Hoff's law formula and a (slope) and b (intercept) is parameters (see: [11] for details). This formula was utilized in this study to determine the different behavior of different cation sources at constant temperatures. In this formula, the (T) is 90˚C and b is 5.5($[Li_{(aq)}]$)$^{-0.0806}$, where $[Li_{(aq)}]$ is in mg/L, and also ($[Li_{(aq)}]$) reflects the Li value transferred to the solution by extraction. The data of previous study were applied to the equation logD_{Li}=-1319/$T_{(K)}$+5.5 ($[Li_{(aq)}]$)$^{-0.0806}$ (see: [11] for details). The calculated logD_{Li} values show an increase as the amount of Li in the solution composition increases. While the calculated value for Cl-$CS_{(NaCl)}$-A and Cl-$CS_{(CaCl2)}$-A solutions are up to 8.4, it is between 7.8 and 8.1 for Cl-$CS_{(FeCl3)}$-A solutions (Table 3) (Figure 5).

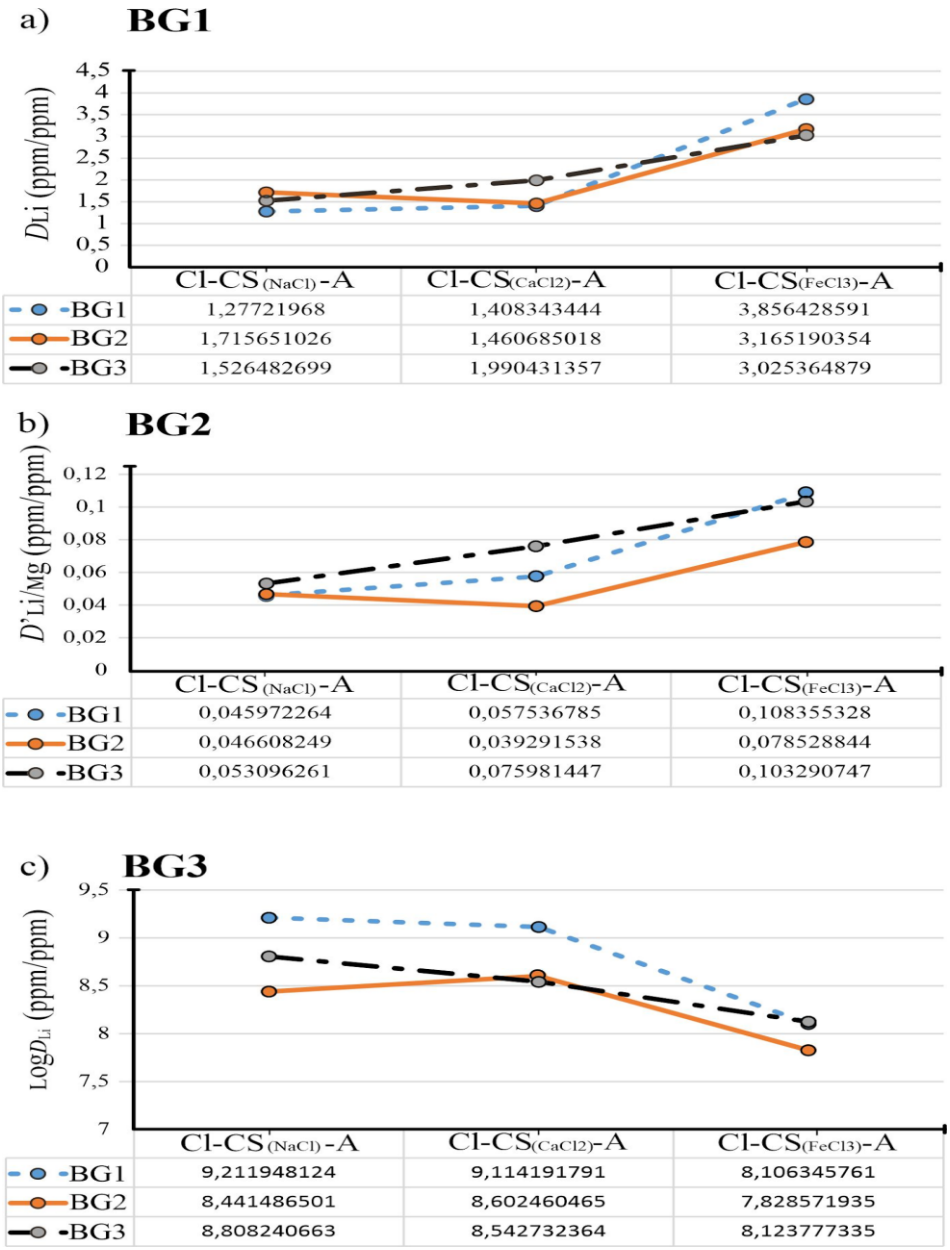

Figure 5. Calculated partition coefficients for lithium content in Cl-CS-A solutions. a: D_{Li} exchange against Cl-$CS_{(NaCl)}$-A, Cl-$CS_{(CaCl2)}$-A and Cl-$CS_{(FeCl3)}$-A solutions, b: $D'_{Li/Mg}$ exchange against Cl-$CS_{(NaCl)}$-A, Cl-$CS_{(CaCl2)}$-A and Cl-$CS_{(FeCl3)}$-A solutions and c: logD_{Li} exchange against Cl-$CS_{(NaCl)}$-A, Cl-$CS_{(CaCl2)}$-A and Cl-CS(FeCl3)-A solutions.

4. DISCUSSION

4.1 Characterization of Clay Mineral

The widening of 001 reflection to approximately 17 Å with the use of ethylene glycol or glycerol in the identification of smectite group clays is one of the most important identification techniques in X-ray diffraction pattern analysis of crystallographically oriented clay minerals. Smectite group is clearly distinguishable from other non-expandable clays with this method [46-48]. [31] and [49] in their characterization studies of clays from the borate zones of Bigadiç; state that the 060 reflectance is >1.52 Å and the 001 reflectance of smectites after treatment ethylene glycol is 17 Å. In this study, after the treatment of the EG, it was determined that the 001 reflection of samples expanded up to 17.45 Å (Figure 3). 001 reflections collapse to almost 9.5 to 10 Å after heating to 400 and 550 C, EG application and heat treatments indicate that the clays investigated are 2:1 smectite clays with swelling properties (Figure 3). The 2:1 type smectites have various cation substitutions in both tetrahedral and octahedral positions and depending on the properties of these cations, smectites are defined as di- and tri-octahedral [46]. The positioning of Mg and Fe (II) and divalent ions in the octahedral structure results in the formation of trioctahedral smectites, whereas the placement of Al and Fe (III) ions in the octahedral structure results in dioctahedral smectites [50-52]. The 060 reflections of samples BG1, BG2 and BG3 were determined to be >1.528 Å in the detailed XRD diffractogram, indicating that these clays can have trioctahedral structures. Mg, which is one of the substantial components of the trioctahedral smectite is constantly found in the interlayer space beside the octahedral structure [50, 51]. The % MgO content of the Li rich clays representing the Bigadiç region was reported to be 23.33% by [31] and 22.5% by [49]. The MgO content of the samples examined in this investigation falls within the range of around 21.85% - 26.08%. The results suggest that the clays found in the Bigadiç region possess a trioctahedral structure and are compatible with the MgO content (27.5%) of raw hectorite [53, 54]. The smectite in the Bigadiç region must have a trioctahedral structure because trioctahedral smectites tend to contain more Li than dioctahedral smectites [55]. Despite several studies suggesting that hectorite should contain a Li_2O content greater than 1.0%, no minimum limit has been established. Using the term 'hectorite' for clay that has less than 1.0% Li_2O is acceptable [55-57]. Studies involving chemical analysis of smectites in the region have revealed that the Bigadiç clays contain Li_2O within the range of 1462 - 3000 ppm [31, 34, 49]. The Li concentration in samples BG1, BG2 and BG3 have recorded 2326.5 ppm, 1446.8 ppm and 1857.2 ppm, respectively (Table 1). Based on the mineralogical and chemical data presented above, it was determined that samples BG1, BG2, and BG3 are hectorite with a 2:1 trioctahedral structure. The key feature of hectorite is the substitution of Li^+ with some of the coordinated states of Mg^{2+} at the octahedral sheets, leading to layer charge and determining the CEC of clays. The CEC of the hectorite ranges from 50 to 150 mmol/100 g in the pH range of 6 to 13 [10]. CEC of the BG1, BG2 and BG3 clays samples were determined as 62 mmol/100 g, 54 mmol/100 g and 52 mmol/100 g, respectively and these values are in agreement with the CEC values observed in raw hectorite.

4.2 Process of the Lithium Extraction

Lithium extraction study conducted on clays from Bigadiç and other borate deposits in the region evaluated chemical processes including the utilization of sulfuric acid and hydrochloric acid, as well as roasting water leaching methods [34, 35, 58, 59]. In this study, unlike previous research, the clay samples were mixed and ground with a cation source before being mixed with acid. Grinding the clay with the cation source increases the specific surface area of the clay. This significantly enhances the ion exchange potential of the charged clay, facilitating the adsorption of the cation onto the clay surface. The extraction of lithium from clays via the ion exchange method relies on the interplay between appropriate cations and the lithium within clay crystal structures. Several studies have demonstrated that organic cations can be included within the interlayer space of hectorite through an ion exchange reaction, in addition to inorganic ions [14-22]. Hectorite has many active sites used for cation exchange, interlayer-, surface-, edge- and inter-particle sites for the ion-exchange reaction. These active sites of clays can easily interact with other

components and cause different types of reactions to occur, so this can be used to change the structure and functionality of hectorite in particular [9].

In this study, three different inorganic salts containing monovalent (NaCl), divalent ($CaCl^2$) and trivalent ($FeCl_3$) ions were applied to raw hectorite samples (BG1, BG2 and BG3). The reason for choosing these three different cation sources is to determine the change in the amount of lithium passing from the crystal structure of hectorite to the solution according to the type of cation source and to calculate the partition coefficient for more interpretable results. According to the results, comparing the Li contents of the solutions after proceses-A+B, the Li contents of the Cl-$CS_{(NaCl)}$-A and Cl-$CS_{(CaCl2)}$-A solution o are quite high compared to Cl-$CS_{(FeCl3)}$-A (Table 1). Although the ionic radii of the Na^+ and Ca^{2+} (102 and 100 pm, respectively, [60]) were larger than those of the Li^+ (76 pm, [60]), the highest lithium content in the end-solution was measured in the $CS_{(NaCl)}$-A and Cl-$CS_{(CaCl2)}$-A solutions. In general, divalent cations be more tend to preferentially to adsorbed on clay exchange zones than monovalent cations, which explains the displacement of the Li^+ against the Ca^{2+} ion and also Li enrichment in solution [11]. The situation is different for monovalent Na^+, and the dominant process in the displacement between Na^+ and Li^+ during the Cl-CS-A interaction is related to the hydration energy of the ions. The hydration energy (ΔH_{Hyd}), which is also correlated with $Z^{2/r}$ (Z = charge on the cation, r = cationic radius (pm)), indicates how strongly an ion attracts water molecules [61, 62]. The larger the atomic size lesser the hydration energy or the energy decreases [63] because the activity coefficient is affected by the radius of the hydrated ion. The ionic diameter of the Na^+ is larger than the Li^+ but the ΔH_{Hyd} of Li^+ (-520 kJ/mol) is higher than that of the Na^+ (-406 kJ/mol). This becomes effective in the Cl-CS-A solution interaction, the transition of lithium from exchangeable positions in the clay crystal lattice into solution and the preferential displacement of these elements. Although the ion radius of Fe^{3+} (64.5 pm) is close to that of Li^+ (76 pm) or even smaller in diameter, the amount of Li^+ in the Cl-$CS_{(FeCl3)}$-A solutions is quite low (Table 1). The fact that Fe^{+3} has a higher ΔH_{Hyd} potential (-4430 kJ/mol) compared to the ΔH_{Hyd} potential of Li^+ (-520 kJ/mol) caused a lower exchange rate of Li^+ and Fe^{3+} in the solution-clay interaction, because as the water cluster binding studies indicate that the ions with high charge densities bind larger water clusters more strongly than those with lower charge densities [62, 64, 65].

The main problem with Li extraction is the presence of both univalent and divalent cations in the clay surface, as this creates significant differences regarding the nature of the exchanger and the concentration of the solution. Bivalent ions are more strongly bound to clay minerals than univalent ions, but this assumption is not valid for Li+ and Mg^{2+}. The diameter of Li^+ (76 pm) is larger than that of Mg^{2+} (72 pm), but the ΔHHyd of Mg^{2+} (-1921 kJ/mol) is higher than that of Li^+ (-520 kJ/mol). The high hydration energy means that when Li^+ and Mg^{2+} bound to the clay surface come into contact with the solution, Mg^{2+} preferentially transfers into the solution more, which is one of the main problems in Li extraction. As a result of the experimental studies carried out as part of this study, it was found that the transition of the Mg^{2+} into solution was significantly lower than that of the Li+. The recovery of lithium from the-CS(NaCl)-A solutions ranges from 58 to 78% and that of magnesium from 3.5 to 2.7% and the ranges from 50 to 71% and that of magnesium from 2.68 to 4.08% for Cl-CS($CaCl_2$)-A solutions when the process-A and B is applied to clays (Table 1). These favorable results show that Mg-poor and Li-rich solutions can be obtained with the addition of Na^+ and Ca^{2+} cation sources to the Bigadiç clays. Detailed explanations about this are given below.

In this study, Li^+ in the exchangeable cation position in the interlayer position of the clay and Li+ in the octahedral sheets were intended, and for this purpose, 1 M H_2SO_4 at 90°C was used in the process-B. The main reason for avoiding the heating process is that heating induces the small cations to migrate out of their interlayer space. When this effect is evaluated by considering Li rich clays, heating of the Li rich clay causes Li^+ to migrate from the interlayer space into the vacant octahedral sites or hexagonal holes of the tetrahedral sheets, or both [66]. [67] have detected that from X-ray photoelectron spectroscopy of Li-Montmorillonite heated at 250 and 350 °C, the Li^+ cations migration from interlayer space to hexagonal and octahedral sites with occupancies of 60 and 40% respectively. In addition, the heating process causes reduction in layer charge, this is called the Hofmann-Klemen effect and refers to the reduction of the layer

charge by heating octahedrally charged smectites saturated with small cations (e.g. Li, Mg, Cu) after heat treatment (when heated to 110°C or more) [66, 68-72]. Acid treatment is one of the most applied solvent extraction methods for the recovery of Li from the hectorite because acid treatment chemically leads to controlled, ion-exchange, and partial dissolution of the hectorite structure. Protonated hectorite is produced by the treatment with mild acid [73, 74], but if the acid is strong enough, the proton strongly attacks the oxygen regions connecting the octahedral and tetrahedral sheets at the edge of the surfaces and partially disrupts the hectorite structure. This increases the specific surface area and average pore volume of the acid-activated hectorite [75-77]. Komadel et al. (1996) [76] indicated that the dissolution rate of Li^+ is slightly higher than that of Mg^{2+} at lower acid concentrations and stated that protons preferentially attack Li^+ octahedra. Based on the above explanations, the fact that the transfer of Li^+ from hectorite to the solution is much higher than the transfer of Mg^{2+} can be interpreted in this study in two ways. i) First, lithium is found in higher concentrations than magnesium in the interlayer position of hectorites. It is supported by the results obtained from Cl-$CS_{(CaCl2)}$-A solutions that lithium is more abundant in the interlayers position of hectorites (The % Mg composition transfer into the solution is much lower than the % Li composition). The application of $CaCl_2$ is a useful methodology for determining interlayer Li^+ quantities or for the separation of lithium from interlayers. [78] and [11] recommended the application of 1 N $CaCl_2$ to eliminate all exchangeable lithium that exists in the interlayer sites of the clays synthesized. ii) Secondly, the Li element located in the octahedral site can show more susceptibility to the acidic process, as mentioned above.

The Mg/Li ratio in the final solution is pivotal in all lithium extraction processes. If the Mg/Li ratio is less than 6, a simple precipitation technique produces a Li-rich precipitate phase and effectively separates Mg from Li. Nonetheless, should the Mg/Li ratio exceed 6, lithium extraction becomes a more arduous [79] and costlier process. Although the Mg/Li ratios of the raw clays (BG1, BG2 and BG3) extracted from the field are higher (>6) the ranges suitable for Li extraction, the Mg/Li ratios of the Cl-$CS_{(NaCl)}$-A and Cl-$CS_{(CaCl2)}$-A solutions are lower than six (<6) (Table 2). The Cl-$CS_{(FeCl3)}$-A solutions have an approximate Mg/Li ratio of 7 to 8. These findings demonstrate that NaCl and $CaCl_2$ can be used as cation sources to attain low Mg/Li ratios (<6) in Bigadiç hetorite. Li-Mg substitution in raw hectorites is constrained to a Li/(Li + Mg) atomic ratio approaching 0.1, according to [80]. [78] found that hectorites with Li concentrations greater than 3600 ppm cannot be obtained experimentally, most likely because it represents the structural limit. At higher content of Li, the structure of the clay becomes unstable and breaks down (when no OH- for F- substitutions occur, [11]. The Li/ (Li + Mg) ratios of BG1, BG2, and BG3 clays are 0.015, 0.009, and 0.013, respectively. These low ratios are linked to the high Mg content present in the clays of the region (Table 3).

DLi partition coefficient calculations were conducted to present the data in a clear and comprehensible way. An apparent decrease in DLi partition coefficient was observed with an increase in Li concentration in the solution, indicating a negative correlation (Table 3) (Figure 5). Such a negative correlation is interpreted as a structural cation substitution occurring during the ion exchange process [11]. As the ratio of Mg/Li in the solution decreased, we observed a decrease in the DLi partition coefficient values. Considering the overall data, an efficiency of 70% or greater from a solution with a Mg/Li ratio below roughly 4 may be achieved by ensuring that the D_{Li} ratio is below about 1.99. For an efficiency of 70%, it is recommended that $D'_{Li/Mg}$ use a partition coefficient value lower than 0.075. All these data was tested with the formula $\log D_{Li} = -1319/T_{(K)} + 5.5 ([Li_{(aq)}])^{-0.0806}$. The findings indicate a direct correlation between the concentration of lithium in the solution and $\log D_{Li}$. This correlation increases at a constant temperature and in relation to the ionic radii [11]. Additionally, for an Mg/Li ratio lower than approximately 6, the $\log D_{Li}$ value should exceed 8.

5. CONCLUSIONS

The importance of lithium deposits worldwide is increasing as lithium is the main component of lithium-ion batteries used in various fields such as electric vehicles and portable devices. In addition, as the need for clean energy solutions grows, lithium plays an important role in renewable energy storage

systems and in the storage of energy from sources such as solar and wind power. As a result, lithium is gaining strategic importance. From Turkey's point of view, it appears to be an important source of lithium in clay deposits. Turkey can benefit economically from this strategic resource through detailed investigation of lithium-rich clays. This study has achieved very important results in terms of bringing clays into the Turkish economy economically and easily.

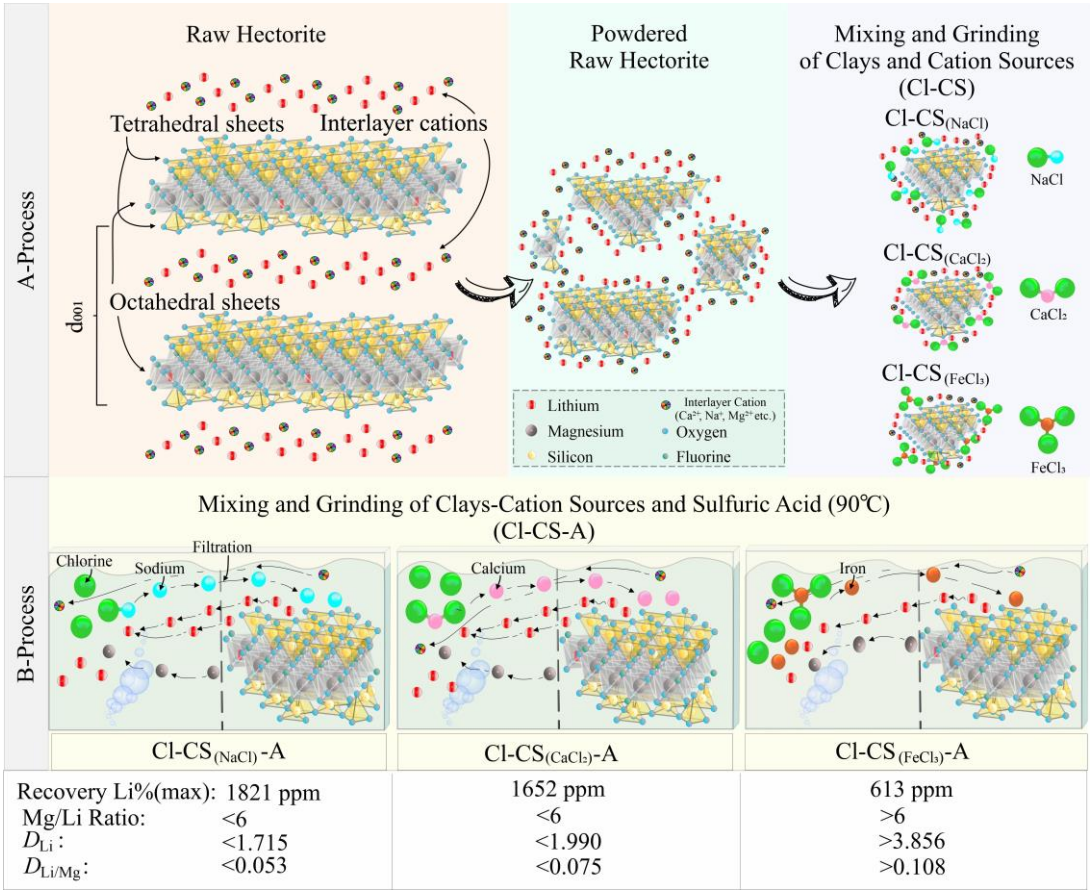

Figure 6. Modal of the lithium extraction process, Process-A(upper): represents powdering raw hectorite, increasing the surface area, grinding and mixing BG1, BG2, BG3 clays with NaCl, $CaCl_2$, and $FeCl^3$ cations and absorbing the cations onto the clay surface. Process-B (below): It represents the mixing of sulfuric acid and clays mixed with cations at 90 ºC and the selective displacement and filtration of cations. Numerical proportions were not considered in the model, and it was drawn without a scale, utilizing the Corel Draw software.

Bigadiç borate basins hold a global recognition for their extensive borate deposits which are often interlayered with Li-rich clay occurrences. Owing to the boost in the global Li demand, investigation of unconventional sources such as clay deposits with the help of technological advancements has become an important task. Within this scope, sets of Cl-CS experiments were conducted on borate basin Li-rich clays using cation sources like NaCl, $CaCl_2$, and $FeCl_3$. Each set has been treated with of H_2SO_4 at a temperature of 90 ºC and filtered. As a result, a solution rich in lithium have been obtained. The processes-A and B are depicted and modelled in Figure 6 without any scaling.

In the results of this study, in which selective cation exchange was aimed, it was found that the Cl(BG1)-CS(NaCl)-A and Cl(BG1)-CS($CaCl_2$)-A solutions of the BG1 sample yielded over 1800 ppm Li with an efficiency exceeding 70%. High concentrations of lithium were also detected in the Cl-CS(NaCl)-A and Cl-CS($CaCl_2$)-A solutions obtained from other experiments. The lithium content in solutions of Cl-CS($FeCl_3$)-A is relatively low which is associated with the hydration enthalpy of Fe^{3+} (Figure 6). One of the most important findings of these investigations is that the transition of Mg into solution from clays

containing large amounts of Mg (between 13 and 15%) is severely limited. The research demonstrated the impact of ion diameters on the extraction of lithium-rich and magnesium-poor solutions from Li-rich clays, and the correlation between hydration enthalpy and Li extraction.

The Mg/Li ratio, which is the easy and economical recovery limit for Li, is <6. This value was approximately obtained in all the Cl-CS-A solutions obtained in this study. The DLi partition coefficient value was calculated to be less than 2.0 and the $D'_{Li/Mg}$ value to be less than 0.075 in solutions with Mg/Li ratios of less than 6. Together with the calculated logD_{Li} value, it was found that the Li content is related to the ionic radius at constant temperature. However, cation exchange reactions in natural environments are highly complicated due to the unpredictability of ion concentration in liquid that passes through clay. Consequently, regional studies and information collected in this study will aid in identifying variations in the reactions of local clays, as well as extracting Li from other Li-rich clay formations worldwide and accurate data interpretation.

Declaration of Competing Interest

The author declares no known financial or personal relationships that could have influenced the work reported in this paper.

Acknowledgements

The author thanks ETİMADEN and Engineer Yasin Yıldız for their hectorite mineral support, and Prof. Dr. Mustafa Topkafa for the provision of laboratory equipment.

Funding

There is no funding for this study.

Data Availability

No data was used for the research described in the article.

REFERENCES

[1] D. C. Bradley, A. D. McCauley, and L. L. Stillings, "Mineral-deposit model for lithium-cesium-tantalum pegmatites," US Geological Survey, 2328-0328, 2017.

[2] T. Bibienne, J.-F. Magnan, A. Rupp, and N. Laroche, "From mine to mind and mobiles: Society's increasing dependence on lithium," Elements: An International Magazine of Mineralogy, Geochemistry, and Petrology, vol. 16, no. 4, pp. 265-270, 2020.

[3] R. J. Bowell, L. Lagos, C. R. de los Hoyos, and J. Declercq, "Classification and characteristics of natural lithium resources," Elements, vol. 16, no. 4, pp. 259-264, 2020.

[4] D. E. Garrett, Handbook of lithium and natural calcium chloride. Elsevier, 2004.

[5] L. Wiklander and M. Elgabaly, "Relative uptake of adsorbed monovalent and divalent cations by excised barley roots as influenced by the exchange capacity," Soil Science, vol. 80, no. 2, pp. 91-94, 1955.

[6] W. Kelley, "Soil properties in relation to exchangeable cations and kinds of exchange material," Soil Science, vol. 98, no. 6, pp. 408-412, 1964.

[7] N. Kumari and C. Mohan, "Basics of clay minerals and their characteristic properties," Clay Clay Miner, vol. 24, pp. 1-29, 2021.

[8] L. Delavernhe, M. Pilavtepe, and K. Emmerich, "Cation exchange capacity of natural and synthetic hectorite," Applied Clay Science, vol. 151, pp. 175-180, 2018.

[9] J. Zhang, C. H. Zhou, S. Petit, and H. Zhang, "Hectorite: Synthesis, modification, assembly and applications," Applied Clay Science, vol. 177, pp. 114-138, 2019.

[10] N. Hegyesi, R. T. Vad, and B. Pukánszky, "Determination of the specific surface area of layered silicates by methylene blue adsorption: The role of structure, pH and layer charge," Applied Clay Science, vol. 146, pp. 50-55, 2017.
[11] A. Decarreau, N. Vigier, H. Pálková, S. Petit, P. Vieillard, and C. Fontaine, "Partitioning of lithium between smectite and solution: An experimental approach," Geochimica et Cosmochimica Acta, vol. 85, pp. 314-325, 2012.
[12] P. Stoffynegli and F. T. Mackenzie, "Mass balance of dissolved lithium in the oceans," Geochimica et Cosmochimica Acta, vol. 48, no. 4, pp. 859-872, 1984.
[13] A. Hamzaoui, A. M'nif, H. Hammi, and R. Rokbani, "Contribution to the lithium recovery from brine," Desalination, vol. 158, no. 1-3, pp. 221-224, 2003.
[14] J. Velasco et al., "Foaming behaviour and cellular structure of LDPE/hectorite nanocomposites," Polymer, vol. 48, no. 7, pp. 2098-2108, 2007.
[15] W. H. Awad et al., "Material properties of nanoclay PVC composites," Polymer, vol. 50, no. 8, pp. 1857-1867, 2009.
[16] L. Yu and P. Cebe, "Crystal polymorphism in electrospun composite nanofibers of poly (vinylidene fluoride) with nanoclay," Polymer, vol. 50, no. 9, pp. 2133-2141, 2009.
[17] L. M. Dykes, J. M. Torkelson, W. R. Burghardt, and R. Krishnamoorti, "Shear-induced orientation in polymer/clay dispersions via in situ X-ray scattering," Polymer, vol. 51, no. 21, pp. 4916-4927, 2010.
[18] A. Walther and A. H. Muller, "Janus particles: synthesis, self-assembly, physical properties, and applications," Chemical reviews, vol. 113, no. 7, pp. 5194-5261, 2013.
[19] H. Tan et al., "ASA-in-water emulsions stabilized by laponite nanoparticles modified with tetramethylammonium chloride," Chemical Engineering Science, vol. 116, pp. 682-693, 2014.
[20] M. Stöter et al., "Controlled exfoliation of layered silicate heterostructures into bilayers and their conversion into giant Janus platelets," Angewandte Chemie, vol. 128, no. 26, pp. 7524-7528, 2016.
[21] M. Daab et al., "Two-step delamination of highly charged, vermiculite-like layered silicates via ordered heterostructures," Langmuir, vol. 33, no. 19, pp. 4816-4822, 2017.
[22] Z. Sun, H. Chen, T. B. Caldwell, and A. M. Thurston, "Selective extraction of lithium from clay minerals," ed: Google Patents, 2021.
[23] B. Sawhney, "Sorption and fixation of microquantities of cesium by clay minerals: effect of saturating cations," Soil Science Society of America Journal, vol. 28, no. 2, pp. 183-186, 1964.
[24] D. Carroll, "Ion exchange in clays and other minerals," Geological Society of America Bulletin, vol. 70, no. 6, pp. 749-779, 1959.
[25] D. Eberl, "Clay mineral formation and transformation in rocks and soils," Philosophical Transactions of the Royal Society of London. Series A, Mathematical and Physical Sciences, vol. 311, no. 1517, pp. 241-257, 1984.
[26] B. B. Velde and A. Meunier, The origin of clay minerals in soils and weathered rocks. Springer Science & Business Media, 2008.
[27] S. C. Aboudi Mana, M. M. Hanafiah, and A. J. K. Chowdhury, "Environmental characteristics of clay and clay-based minerals," GeoloGy, ecoloGy, and landscapes, vol. 1, no. 3, pp. 155-161, 2017.
[28] F. Anouar, A. Elmchaouri, N. Taoufik, and Y. Rakhila, "Investigation of the ion exchange effect on surface properties and porous structure of clay: Application of ascorbic acid adsorption," Journal of Environmental Chemical Engineering, vol. 7, no. 5, p. 103404, 2019.
[29] G. Ataman and O. Baysal, "Clay mineralogy of Turkish borate deposits," Chemical Geology, vol. 22, pp. 233-247, 1978.
[30] C. Helvaci, "Stratigraphy, mineralogy, and genesis of the Bigadiç borate deposits, Western Turkey," Economic Geology, vol. 90, no. 5, pp. 1237-1260, 1995.
[31] C. Helvaci, H. Mordogan, M. Çolak, and I. Gündogan, "Presence and distribution of lithium in borate deposits and some recent lake waters of west-central Turkey," International Geology Review, vol. 46, no. 2, pp. 177-190, 2004.

[32] M. m. Çolak, C. Helvaci, and M. Maggetti, "Saponite from the Emet colemanite mines, Kutahya, Turkey," Clays and Clay Minerals, vol. 48, no. 4, pp. 409-423, 2000.
[33] B. Ertan and Y. Erdoğan, "Emet-Espey bölgesindeki borlu killerde eser element tayini," Journal of Science and Technology of Dumlupınar University, no. 033, pp. 25-32, 2014.
[34] W.-J. Lee et al., "Lithium extraction from smectitic clay occurring in lithium-bearing boron deposits in Turkey," Journal of the Mineralogical Society of Korea, vol. 29, no. 4, pp. 167-177, 2016.
[35] A. Obut, İ. Ehsani, Z. Aktosun, A. Yörükoğlu, İ. Girgin, A. Temel and H. Deveci, "Leaching behaviour of lithium from a clay sample of Kırka borate deposit in sulfuric acid solutions," Journal of Boron, vol. 5, no. 4, pp. 170-175, 2020.
[36] H. Şensöz, Z. E. Sayın, M. Savaş, and Y. Erdoğan, "Emet Bor Üretim Tesisleri Atıklarının Lityum İçeriğinin İncelenmesi," Afyon Kocatepe Üniversitesi Fen Ve Mühendislik Bilimleri Dergisi, vol. 21, no. 6, pp. 1460-1469, 2021.
[37] H. Mordoğan, M. Akdağ, and C. Helvacı, "Lithium recover from low-grade lithium-bearing clays by H2SO4 and roast-water leach processes," Geosound (Yerbilimleri), vol. 24, pp. 141-150, 1994.
[38] C. Helvacı and O. Alaca, "Geology and Mineralogy of the Bigadiç Borate Deposıts and Vicinity," Bulletin of the Mineral Research and Exploration, vol. 113, no. 113, pp. 31-63, 1991.
[39] A. I. Okay, "Was the Late Triassic orogeny in Turkey caused by the collision of an oceanic plateau?," Geological Society, London, Special Publications, vol. 173, no. 1, pp. 25-41, 2000.
[40] İ. Koçak and Ş. Koç, "Trace element contents of Bigadiç and Kestelek borate deposits," to Boron, p. 232, 2011.
[41] İ. Koçak and Ş. Koç, "Major and trace element geochemistry of the Bigadiç Borate deposit, Balikesir, Turkiye," Geochemistry International, vol. 50, pp. 926-951, 2012.
[42] Y. Y. Öztürk, A. Selin, and C. Helvacı, "Bor Minerallerinin Duraylı İzotop Jeokimyası: Bigadiç (Balıkesir) Borat Yatağından Bir Örnek," Yerbilimleri, vol. 35, no. 1, pp. 141-168, 2014.
[43] Y. Dilek and Ş. Altunkaynak, "Geochemical and temporal evolution of Cenozoic magmatism in western Turkey: mantle response to collision, slab break-off, and lithospheric tearing in an orogenic belt," Geological Society, London, Special Publications, vol. 311, no. 1, pp. 213-233, 2009.
[44] F. Gulmez, H. U. Ercan, N. Lom, G. Gocmengil, and E. Damci, "The inherited structure of the Gediz Graben (Aegean Extensional Province, Turkey): insights from the deep geothermal wells in the Alasehir sub-basin," International Journal Of Earth Sciences, 2023.
[45] S. İşçi, "Kil/PVA ve organokil/PVA nanokompozitlerin sentezi ve karakterizasyonu," Fen Bilimleri Enstitüsü, 2007.
[46] G. Brown, Crystal structures of clay minerals and their X-ray identification. The mineralogical society of Great Britain and Ireland, 1982.
[47] D. M. Moore and R. C. Reynolds Jr, X-ray Diffraction and the Identification and Analysis of Clay Minerals. Oxford University Press (OUP), 1989.
[48] S. Yamashita, H. Mukai, N. Tomioka, H. Kagi, and Y. Suzuki, "Iron-rich smectite formation in subseafloor basaltic lava in aged oceanic crust," Scientific Reports, vol. 9, no. 1, p. 11306, 2019.
[49] S. Kadir, T. Külah, H. Erkoyun, C. Helvacı, M. Eren, and B. Demiral, "Mineralogy, geochemistry, and genesis of lithium-bearing argillaceous sediments associated with the Neogene Bigadiç borate deposits, Balıkesir, western Anatolia, Türkiye," Applied Clay Science, vol. 242, p. 107015, 2023.
[50] M. D. Foster, "The importance of exchangeable magnesium and cation-exchange capacity in the study of montmorillonitic clays," American Mineralogist: Journal of Earth and Planetary Materials, vol. 36, no. 9-10, pp. 717-730, 1951.
[51] J. Mering, "Smectites," in Soil Components: Vol. 2: Inorganic Components: Springer, 1975, pp. 97-119.
[52] S. Petit, A. Decarreau, W. Gates, P. Andrieux, and O. Grauby, "Hydrothermal synthesis of dioctahedral smectites: The Al–Fe3+ chemical series. Part II: Crystal-chemistry," Applied Clay Science, vol. 104, pp. 96-105, 2015.

[53] Y. Tardy, G. Krempp, and N. Trauth, "Le lithium dans les minéraux argileux des sédiments et des sols," Geochimica et Cosmochimica Acta, vol. 36, no. 4, pp. 397-412, 1972.
[54] A. Decarreau, "Cristallogènese expérimentale des smectites magnésiennes: Hectorite, stévensite," Bulletin de minéralogie, vol. 103, no. 6, pp. 579-590, 1980.
[55] H. C. Starkey, The role of clays in fixing lithium (no. 1278). US Government Printing Office, 1982.
[56] C. S. Ross and S. B. Hendricks, Minerals of the montmorillonite group: Their origin and relation to soils and clays (no. 205). US Government Printing Office, 1945.
[57] E. F. Brenner-Tourtelot and R. K. Glanzman, "Lithium-bearing rocks of the horse spring formation, Clark County, Nevada," in Lithium Needs and Resources: Elsevier, 1978, pp. 255-262.
[58] H. J. Koo, B. Y. Lee, H. G. Cho, and S. M. Koh, "Study of Heat and Acid Treatment for Hectorite in Turkey Boron Deposit," Journal of the Mineralogical Society of Korea, vol. 29, no. 3, pp. 103-111, 2016.
[59] A. Obut, Z. Aktosun, İ. Girgin, H. Deveci, and A. Yörükoğlu, "Characterization and treatment of clayey waste using a sulfuric acid roasting-water leaching process for the extraction of lithium," Physicochemical Problems of Mineral Processing, vol. 58, no. 4, 2022.
[60] R. D. Shannon, "Revised effective ionic radii and systematic studies of interatomic distances in halides and chalcogenides," Acta crystallographica section A: crystal physics, diffraction, theoretical and general crystallography, vol. 32, no. 5, pp. 751-767, 1976.
[61] K. Birdi, Handbook of surface and colloid chemistry. CRC press, 2008.
[62] B. Tansel, "Significance of thermodynamic and physical characteristics on permeation of ions during membrane separation: Hydrated radius, hydration free energy and viscous effects," Separation and purification technology, vol. 86, pp. 119-126, 2012.
[63] B. J. Teppen and D. M. Miller, "Hydration energy determines isovalent cation exchange selectivity by clay minerals," Soil Science Society of America Journal, vol. 70, no. 1, pp. 31-40, 2006.
[64] M. W. Washabaugh and K. D. Collins, "The systematic characterization by aqueous column chromatography of solutes which affect protein stability," Journal of Biological Chemistry, vol. 261, no. 27, pp. 12477-12485, 1986.
[65] J. Havel and E. Högfeldt, "Evaluation of water sorption equilibrium data on Dowex ion exchanger using WSLET-MINUIT program," Scripta Fac. Sci. Nat. Univ. Masaryk. Brun. Chem, vol. 25, pp. 73-84, 1995.
[66] P. R. Bodart, L. Delmotte, S. Rigolet, J. Brendlé, and R. D. Gougeon, "7Li {19F} TEDOR NMR to observe the lithium migration in heated montmorillonite," Applied Clay Science, vol. 157, pp. 204-211, 2018.
[67] T. Ebina, T. Iwasaki, And A. Chatterjee, "XPS and DFT study on the migration of lithium in montmorillonite," Clay science, vol. 10, no. 6, pp. 569-581, 1999.
[68] U. Hofmann and R. Klemen, "Verlust der austauschfähigkeit von lithiumionen an bentonit durch erhitzung," Zeitschrift für anorganische Chemie, vol. 262, no. 1-5, pp. 95-99, 1950.
[69] R. Greene-Kelly, "A test for montmorillonite," Nature, vol. 170, no. 4339, pp. 1130-1131, 1952.
[70] R. Tettenhorst, "Cation migration in montmorillonites," American Mineralogist: Journal of Earth and Planetary Materials, vol. 47, no. 5-6, pp. 769-773, 1962.
[71] P. Komadel, J. Madejová, and J. Bujdák, "Preparation and properties of reduced-charge smectites—a review," Clays and Clay Minerals, vol. 53, pp. 313-334, 2005.
[72] B. K. G. Theng, Formation and properties of clay-polymer complexes. Elsevier, 2012.
[73] I. Tkáč, P. Komadel, and D. Müller, "Acid-treated montmorillonites—a study by 29Si and 27Al MAS NMR," Clay Minerals, vol. 29, no. 1, pp. 11-19, 1994.
[74] C. Breen, J. Madejová, and P. Komadel, "Characterisation of moderately acid-treated, size-fractionated montmorillonites using IR and MAS NMR spectroscopy and thermal analysis," Journal of Materials Chemistry, vol. 5, no. 3, pp. 469-474, 1995.
[75] B. R. Bickmore, D. Bosbach, M. F. Hochella Jr, L. Charlet, and E. Rufe, "In situ atomic force microscopy study of hectorite and nontronite dissolution: Implications for phyllosilicate edge

surface structures and dissolution mechanisms," American Mineralogist, vol. 86, no. 4, pp. 411-423, 2001.

[76] P. Komadel, "Acid activated clays: Materials in continuous demand," Applied Clay Science, vol. 131, pp. 84-99, 2016.

[77] F. Franco, M. Pozo, J. A. Cecilia, M. Benitez-Guerrero, and M. Lorente, "Effectiveness of microwave assisted acid treatment on dioctahedral and trioctahedral smectites. The influence of octahedral composition," Applied Clay Science, vol. 120, pp. 70-80, 2016.

[78] N. Vigier, A. Decarreau, R. Millot, J. Carignan, S. Petit, and C. France-Lanord, "Quantifying Li isotope fractionation during smectite formation and implications for the Li cycle," Geochimica et Cosmochimica Acta, vol. 72, no. 3, pp. 780-792, 2008.

[79] Z. Zhao, X. Si, X. Liu, L. He, and X. Liang, "Li extraction from high Mg/Li ratio brine with LiFePO4/$FePO_4$ as electrode materials," Hydrometallurgy, vol. 133, pp. 75-83, 2013.

[80] G. t. Brown and G. Brindley, "X-ray diffraction procedures for clay mineral identification," 1980.